


Quzhou Aurantii Fructus Flavonoids Ameliorate Inflammatory Responses, Intestinal Barrier Dysfunction in DSS-Induced Colitis by Modulating PI3K/AKT Signaling Pathway and Gut Microbiome

Haiou Wang¹, Wenkang Huang¹, Xiaoya Pan¹, Meizi Tian¹, Jiahui Chen¹, Xiaotong Liu¹, Qin Li¹, Jianhua Qi², Yiping Ye¹, Lijuan Gao¹ 

¹School of Pharmacy, Hangzhou Medical College, Hangzhou, 310013, People's Republic of China; ²College of Pharmaceutical Sciences, Zhejiang University, Hangzhou, People's Republic of China

Correspondence: Lijuan Gao; Yiping Ye, Hangzhou Medical College, 182 Tianmushan Road, Hangzhou, Zhejiang, 310013, People's Republic of China, Email gaolijuan04141002@126.com; yeyiping2005@163.com

Purpose: To explore the protective effect and underlying mechanism of Quzhou Aurantii Fructus flavonoids (QAFF) on Ulcerative colitis (UC).

Methods: The constituents of QAFF were accurately determined by ultra-performance liquid chromatography-tandem mass spectrometry (UPLC-MS/MS). The therapeutic impacts of QAFF were assessed in dextran sulfate sodium (DSS)-induced UC mice, focusing on the changes in body weight, disease activity index (DAI), colon length, histological assessment of colonic tissues, levels of pro-inflammatory cytokines, and expression of tight junction proteins. Western blotting confirmed key regulatory proteins within the differential signaling pathways, guided by transcriptome analysis. Additionally, the influence of QAFF on the gut microbiome was explored through 16S ribosomal RNA (rRNA) sequencing. The alterations in endogenous metabolites were detected by untargeted metabolomics, and their potential correlation with intestinal flora was then examined utilizing Spearman correlation analysis. Subsequently, the regulation of gut microbiome by QAFF was validated by fecal microbiota transplantation (FMT).

Results: Eleven flavonoids, including Naringin and hesperidin, were initially identified from QAFF. In vivo experiments demonstrated that QAFF effectively ameliorated colitis symptoms, reduced IL-6, IL-1 β , and TNF- α levels, enhanced intestinal barrier integrity, and down-regulated PI3K/AKT pathway activation. Furthermore, QAFF elevated the levels of beneficial bacteria like *Lachnospiraceae_NK4A136_group* and *Alloprevotella* and concurrently reduced the pathogenic bacteria such as *Escherichia-Shigella*, *[Eubacterium]_siraecum_group*, and *Parabacteroides*. Metabolomics analysis revealed that 34 endogenous metabolites exhibited significant alterations, predominantly associated with Glycerophospholipid metabolism. These metabolites were significantly correlated with those differential bacteria modulated by QAFF. Lastly, the administration of QAFF via FMT ameliorated the colitis symptoms.

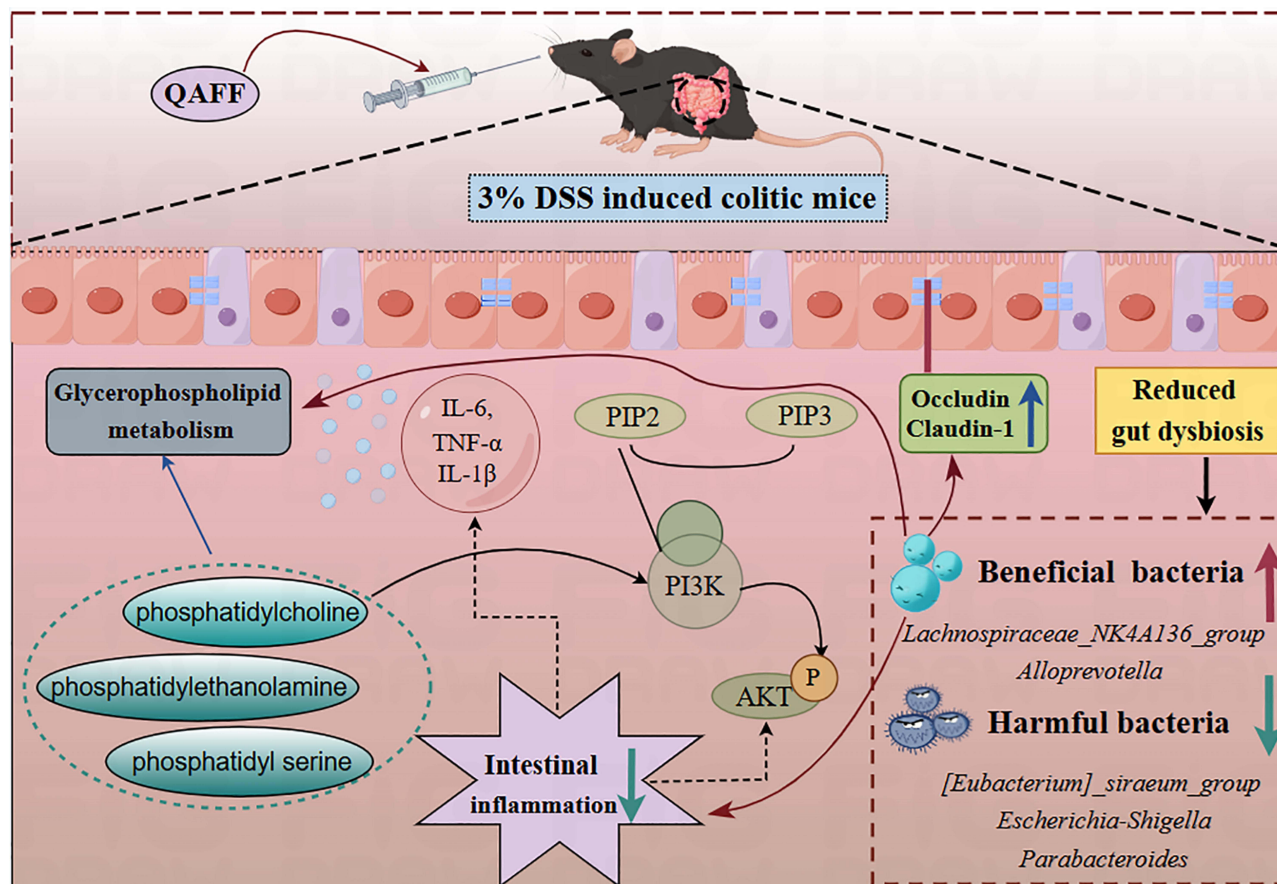
Conclusion: QAFF could ameliorate inflammatory responses and intestinal barrier dysfunction in DSS-induced UC mice probably by modulating the PI3K/AKT signaling pathway and gut microbiome, offering promising evidence for the therapeutic potential of QAFF in UC treatment.

Keywords: Quzhou Aurantii Fructus flavonoids, Ulcerative colitis, inflammation, Gut microbiota, PI3K/AKT, Fecal microbiota transplantation

Introduction

Ulcerative colitis (UC) is a chronic, non-specific inflammatory bowel disease (IBD) primarily affecting the rectum and colon. It is characterized by distinctive symptoms such as diarrhea, hematochezia, frequent relapses that can lead to an increased risk of colorectal cancer.¹ The incidence and prevalence of UC are rising globally, with significant increases observed in Asia.² UC typically manifests in two peak age ranges of onset: between 20–30 years and between 50–80

Graphical Abstract



years, with a recent trend towards earlier disease onset.³ Current treatment options include 5-aminosalicylic acid preparations, oral thiopurines, immunosuppressive agents, biologics, as well as oral small molecules including tofacitinib and ozanimod, and corticosteroids. However, these therapies may not always achieve remission and even have significant adverse reactions.⁴ Therefore, developing more effective and safer therapeutic options is crucial to address this unmet medical need.

Various factors have been identified to contribute to the development of UC, including genetics, environmental influences, disruptions in signaling pathways, compromised intestinal barrier function, mitochondrial dysfunction, and gut microbiome imbalances.⁵ Among these, the modulation of various signaling pathways, such as the phosphatidylinositol 3-kinase (PI3K)/protein kinase B (PI3K/AKT), the Janus kinase (JAK)-signal transducer and activator of transcription (STAT), the mitogen-activated protein kinase (MAPK), and the nuclear factor-κB (NF-κB) pathways, provides a new perspective for the treatment of UC.⁶ Additionally, gut microbiota plays an important role in maintaining host health through the regulation of intestinal metabolism and suppression of pathogenic microorganisms.⁷ However, disruption of the intestinal microbiome composition and function is closely linked to UC development.⁸ Individuals with UC exhibited a reduced abundance and diversity of gut microbiome compared to healthy individuals, with a notable imbalance in the major phyla *Firmicutes* and *Bacteroidota*.⁹ This imbalance negatively affects the integrity of intestinal epithelial cell barrier, resulting in increased permeability and exacerbating intestinal inflammation.¹⁰ Recently, research has increasingly focused on herbal plants as potential treatments for UC, modulating multiple pathways through multi-target approaches to alleviate symptoms and inflammatory responses. Furthermore, several studies have indicated that the

therapeutic effects of herbal plants on metabolic diseases are closely linked to gut microbiota, highlighting their potential significance in the development of new treatment strategies for UC.^{6,11} *Hericium erinaceus*, a fungus of Chinese origin is already utilized clinically as nutraceutical supplementation for the treatment of UC, exerting promising efficacy through a variety of mechanisms.¹²

Quzhou Aurantii Fructus (QAF), the dried immature fruit of *Citrus changshan-huyou* Y.B. Chang, is a widely recognized variety of Aurantii Fructus (AF) traditionally used in China to treat gastrointestinal disorders.¹³ It possesses similar properties to AF, which is well-known for Qi-regulating and depression-dispersing effects. Studies have demonstrated that the flavonoid extract of QAF (QAF Flavonoids, QAFF) effectively reduces obesity, inflammation, and liver steatosis, playing a critical role in combating obesity and related metabolic diseases.¹⁴ The key flavonoids identified in QAFF include naringin, narirutin, hesperidin, and neohesperidin, which are acknowledged as potential antioxidants and anti-inflammatory agents.¹⁵ However, the pharmacological impacts and intricate mechanisms of action of QAFF are yet to be fully uncovered and comprehended.

The present study explored the therapeutic efficacy of QAFF in the context of UC. Initially, QAFF components were extracted and identified from Quzhou Aurantii Fructus. Subsequently, their pharmacological effects were assessed in DSS-treated UC mice. To elucidate the potential mechanisms of action, comprehensive approaches were employed, encompassing transcriptomics analysis, 16S rRNA sequencing, untargeted metabolomics, and verification by Western blotting. Additionally, a fecal microbiota transplantation (FMT) experiment was conducted to substantiate the hypothesis that QAFF alleviates DSS-induced colitis via the modulation of gut microbiota. This investigation provides a pharmacodynamic foundation for the development of novel UC treatments.

Materials and Methods

Materials and Reagents

QAF decoction pieces were obtained from Changshan Tiandao Chinese Medicine Slices Co. Ltd. (Zhejiang, China). DSS (molecular weight: $3.6\text{--}5.0 \times 10^4$ Da) was sourced from Meilun Biotechnology Co. Ltd. (Dalian, China). 5-ASA was obtained from Aladdin (Shanghai, China). Enzyme-linked immunosorbent assay (ELISA) kits were procured from Shanghai Enzyme-linked Biotechnology (Shanghai, China). Primary antibodies for Occludin, Claudin-1, and Zonula occludens-1 (ZO-1) were purchased from Abcam (Cambridge, United Kingdom). Antibodies against PI3 Kinase p85 (PI3K), Phospho-PI3 Kinase p85 (P-PI3K), phosphorylated-AKT (P-AKT), and AKT were procured from Cell Signaling Technology (Massachusetts, USA). β -actin and GAPDH antibodies were acquired from Abbkine (Wuhan, China). Secondary antibodies were gained from Beyotime Biotechnology (Shanghai, China). Neomycin sulfate, metronidazole, ampicillin sodium, and vancomycin hydrochloride were purchased from Macklin (Shanghai, China).

Preparation of QAFF

QAFF was prepared by extracting 1.1 kg of dried decoction pieces of QAF with 65% ethanol thrice for 1.5 hours each. The resulting solution was filtered and then concentrated to yield 175 g of extract. Subsequently, the extract was purified using AB-8 macroporous resins. The elution was performed with H₂O, 20% aqueous ethanol, and 50% aqueous ethanol. The desired fraction eluted with 50% aqueous ethanol was further concentrated and freeze-dried to obtain QAFF (91.9 g).

UPLC-MS/MS Analysis

The qualitative analysis of flavonoid components in QAFF was performed using UPLC-MS/MS. This technique enabled identifying and characterizing specific flavonoids presented in the extract. The established protocols were employed for this study according to our previous research.¹⁵

DSS-Induced UC Mouse Model

Male C57BL/6J mice with six-week-old (weight 18–22 g) were sourced from the Zhejiang Province Experimental Animal Center. The facility holds licenses and certifications for laboratory animals, including SCXK (Zhejiang)

2019–0002 and SYXK (Zhejiang) 2019–0011. All procedures strictly adhered to the Guidelines for the Care and Use of Laboratory Animals.

After a one-week acclimatization period, the mice were randomly divided into six groups ($n = 6/\text{group}$). The control group (Ctrl), model group induced by 3% DSS (DSS, w/v), DSS with varying dosages of QAFF (50, 100, and 200 mg/kg), and DSS with 5-ASA (200 mg/kg) as a positive control. QAFF and 5-ASA were administered daily via oral gavage for 11 days. The control group received sterile water instead. Throughout the treatment period (days 4–11), all groups except the control group were provided with unrestricted access to drinking water containing 3% DSS. Daily food and water consumption were measured to assess any significant differences between the groups.

Assessment of Symptoms of UC Progression

Body weight, dietary intake, water intake, fecal consistency, and degree of hematochezia were monitored daily. Based on these observations, the disease activity index (DAI) was evaluated, following the protocols outlined in [Table S1](#) with minor modifications as detailed in the same table.¹⁶ At the experiment's conclusion, all mice were humanely euthanized, and samples from the colon and cecum were harvested for analysis. Colon length was then measured.

Histomorphometric Analysis

A histopathological assessment of colonic damage was performed using hematoxylin and eosin (H&E) staining according to established protocols. Briefly, colonic tissues were washed with phosphate-buffered saline (PBS) and soaked in a 10% neutral formalin solution. The tissues were further embedded in paraffin wax, sectioned into thin slices, and stained with H&E for microscopic observation. Tissue sections were then scored based on established criteria ([Table S2](#)) to evaluate the changes in epithelial morphology and the severity of inflammatory infiltration.¹⁷ The combined histological score, ranging from 0 to 8, was determined by summing the individual scores for epithelial morphology and inflammatory infiltrate.

RNA Sequencing (RNA-Seq)

RNA was extracted using the magnetic bead method. The quality of the extracted RNA was assessed using the Agilent 2100 Bioanalyzer. Sequencing libraries were designed to ensure consistency and reproducibility. For next-generation sequencing, the Illumina NovaSeq 6000 platform was chosen, generating 150 nt paired-end reads to enhance coverage and resolution. HISAT2 was employed for alignment with the mouse reference genome. Differentially expressed genes (DEGs) were identified using DESeq2, applying the criteria of $q\text{-value} < 0.05$ and fold change > 2 or < 0.5 ($|\log_2\text{FC}| > 1$). Additionally, principal component analysis (PCA) analysis, Volcano maps and gene set enrichment analysis (GSEA) were performed on the Ouyi Bio Cloud platform (<https://cloud.oebiotech.com>). Differential gene functions among groups were predicted by edgeR based on Kyoto Encyclopedia of Genes and Genomes (KEGG).¹⁸ GSEA focuses on the changes of gene sets with consistent differences under specific biological conditions, and comprehensively considers those genes with insignificant differential expression but important biological significance.¹⁹ Therefore, the whole detected genes were subjected to GSEA using gene set knowledge base (GSKB). Leading-edge gene sets (LEGSs) were screened based on $|\text{Normalized enrichment score (NES)}| > 1$, $P < 0.05$, and false discovery rate (FDR) < 0.25 .²⁰

ELISA Analysis

The colorectal tissues were homogenized following grinding, and then mixed with PBS. The supernatant of each group was obtained by centrifugation at 12,000 rpm for 10 min at 4 °C. The levels of pro-inflammatory cytokines, such as IL-1 β , IL-6, and TNF- α , were then assessed in the supernatant using ELISA kits following the protocols.

Western Blot Analysis

Colon tissues were homogenized to extract total protein using RIPA lysis buffer supplemented with phosphatase and protease inhibitors (Beyotime Biotechnology, China). The homogenate was then centrifuged at 4 °C, 12,000 rpm for 30 min. The protein concentration obtained from the supernatant was detected using a BCA kit. The denatured proteins were then separated by SDS-PAGE and transferred onto PVDF membranes (Merck, USA). The membranes were blocked

and subsequently incubated with primary antibodies overnight at 4 °C, then incubated with the secondary antibodies for 2 h. Finally, the protein expression levels were visualized using a Fusion-FX6 imaging system (Vilber, France) and quantified using Evolution-Capt Edge software.

Immunohistochemistry Analyses

Paraffin-embedded colon tissues were dewaxed using water, an eco-friendly dewaxing agent, and a graded alcohol series. Antigen retrieval was then performed. Following inhibition of endogenous peroxidase activity, tissue sections were blocked with 10% goat serum for 30 min to minimize non-specific antibody binding. The primary antibody was subsequently applied to the tissue sections and incubated overnight at 4 °C after removing the serum. The sample sections were then washed thrice with TBST before being incubated with the secondary antibody for 45 min. Following washes, the sample sections were stained with 3,3'-diaminobenzidine tetrahydrochloride (DAB) and hematoxylin. After washing, hydrochloric acid-ethanol differentiation was performed for 1–2s. Finally, the sections were washed again, mounted on slides, and examined under a light microscope for nuclear staining.

16S rRNA Sequencing and Bioinformatics Analyses

The contents of the collected cecum were rapidly frozen in liquid nitrogen and then stored at −80 °C.

Bacterial genomic DNA from bacterial samples was extracted using a commercially available DNA extraction kit according to the protocol. The extracted DNA was used as a template for polymerase chain reaction (PCR) amplification of the 16S ribosomal RNA (rRNA) genes of the bacteria. Takara Ex Taq and barcoded primers were utilized for the amplification. Universal primers 343F (5'-TACGGRAGGCAGCAG-3') and 798R (5'-AGGGTATCTAATCCT-3') were employed to specifically amplify the V3-V4 regions of the 16S rRNA genes, a region informative for assessing bacterial diversity. The quality of the amplicons was verified using gel electrophoresis, purified by AMPure XP beads, and then quantified employing the Qubit dsDNA assay kit. Finally, the purified amplicons underwent paired-end sequencing on an Illumina platform, with library construction and sequencing performed by Shanghai Ouyi Biomedical Technology Co. Alpha diversity, principal coordinate analysis (PCoA), Linear discriminant analysis Effect Size (LEfSe) analysis, and histograms were performed using Ouyi Bio Cloud platform (<https://cloud.oebiotech.com>). The difference between the two samples was analyzed by SPSS Statistics 23.

Metabolomic Analysis

LC-MS/MS metabolomics of colon tissues was performed by Shanghai Lu-Ming Biotech Co. The specific conditions are described in the Supplementary Material 1. The LC-MS data obtained were analyzed utilizing Progenesis QI V2.3 software (Nonlinear, Dynamics, Newcastle, UK). Metabolite identification was facilitated through The Human Metabolome Database (HMDB), Lipidmaps (V2.3), Metlin, and self-constructed databases. Compounds were identified based on their precise mass-to-charge ratios (M/z), secondary fragmentation patterns, and isotopic distributions. The partial least squares discriminant analysis (PLS-DA) was performed to discriminate observations between groups. Differential metabolites were selected for further biological analysis by employing a two-partition approach that considered both the variable importance in projection (VIP) value > 1 and *P*-value < 0.05. Volcano plots were generated based on log2 (fold change) of differential metabolites. The common differential metabolites of DSS vs Ctrl and QAFF-L vs DSS were plotted using Venn diagrams, normalized, and plotted using clustered heatmaps. The shared differential metabolites were anatomized by KEGG pathway enrichment analysis. The above biological analyses were presented on the Ouyi BioCloud platform (<https://cloud.oebiotech.com>).

Correlation Analysis

Correlations were determined using the Spearman correlation method on the Ouyi Bio Cloud platform (<https://cloud.oebiotech.com>).

Fecal Microbiota Transplantation (FMT)

The cecal transplantation procedure was executed adhering to the previously reported protocols.²¹ Briefly, male C57BL/6 donor mice (6 weeks; 18–22 g) were randomized into 2 groups ($n = 10/\text{group}$): the DSS and QAFF treatment groups. The QAFF group received a daily gavage of 50 mg/kg (0.2 mL/mouse), whereas the DSS group was given equal distilled water. From day 4 to day 11, both groups were given drinking water containing 3% DSS. Feces from donor mice were collected separately starting from day 10 to day 11, frozen immediately, and stored at -80°C . The fecal samples from each group were combined, diluted 1:10 (w/v, g/mL) in sterile saline, vortexed for 5 min to ensure homogeneity, and centrifuged at 4000 rpm for 5 min at 4°C . Finally, the resulting supernatant was collected as the transplant material.

Fifteen male C57BL/6 mice were allocated into 3 groups randomly ($n = 5/\text{group}$): control (Ctrl), DSS-DSSfe, and DSS-QAFFfe. All mice received oral gavage with a combination of neomycin sulfate at 200 mg/kg, metronidazole at 200 mg/kg, ampicillin sodium at 200 mg/kg, and vancomycin hydrochloride at 100 mg/kg for five days to deplete intestinal microorganism.²² The Ctrl group received an equivalent volume of distilled water, while the remaining groups consumed water containing 3% DSS to induce acute colitis from day 6 to day 13. Simultaneously, these groups were supplemented with a daily fecal microbiota solution (0.2 mL/mouse) for eight days.

Statistical Analysis

Results are expressed as mean \pm standard deviation (SD). The experimental data were examined for their statistically differences using One-way analysis of variance (ANOVA) and t -tests. The P -values of less than 0.05 were statistically significant. The calculations and graphs were employed with GraphPad Prism 8.0 software.

Results

Identification and Detection of QAFF

UPLC-MS/MS analysis was employed for a comprehensive characterization of the flavonoid components in QAFF. The analysis identified eleven flavonoid components in the negative ion chromatogram (Figure 1) were listed in Table S3. These key compounds included Eriocitrin (M1), Neoeriocitrin (M2), Naringin 6"-rhamnoside (M3), Hesperetin 5-O-glucoside (M4), Narirutin (M5), hesperetin 7-(2,6-dirhamnosyl)glucoside (M6), Naringin (M7), Hesperidin (M8), Neohesperidin (M9), brutieridin (M10), and Poncirin (M11). According to the standard substances, the total content of four key flavonoid components, Narirutin, Naringin, Hesperidin, and Neohesperidin, constituted 78.8% of QAFF through HPLC analysis (Table S4), highlighting their predominance in the overall flavonoid profile.

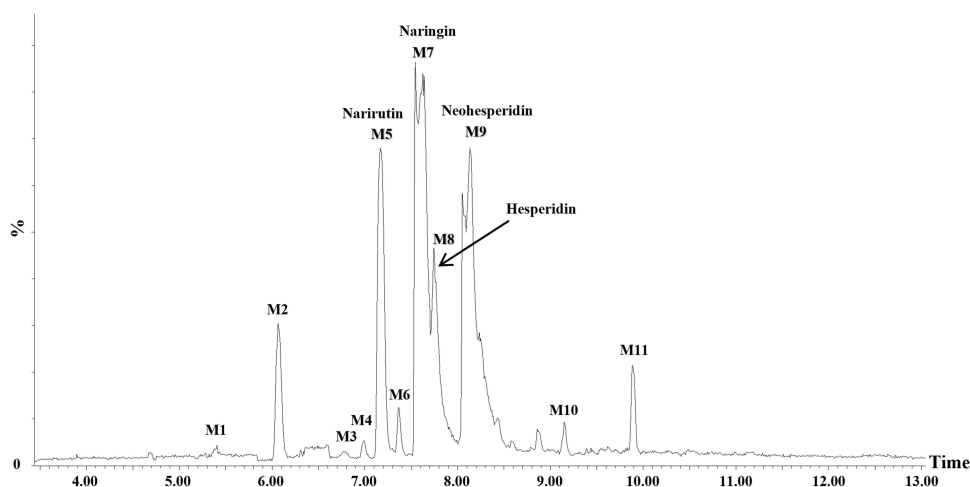


Figure 1 The negative ion chromatography of UPLC-MS/MS of QAFF.

QAFF Dampened DSS-Induced UC in Mice

To evaluate the protective effects of prophylactic QAFF supplementation against UC, mice were orally administered a 3% DSS solution following QAFF treatment for three days (Figure 2A). Mice treated with DSS developed symptoms including diarrhea, decreased activity, poor fur condition, and dysphoria on the sixth day. Fecal occult blood was observed on the eighth day, confirming successful colitis induction by 3% DSS. At the experiment's conclusion, the DSS-induced group exhibited significant

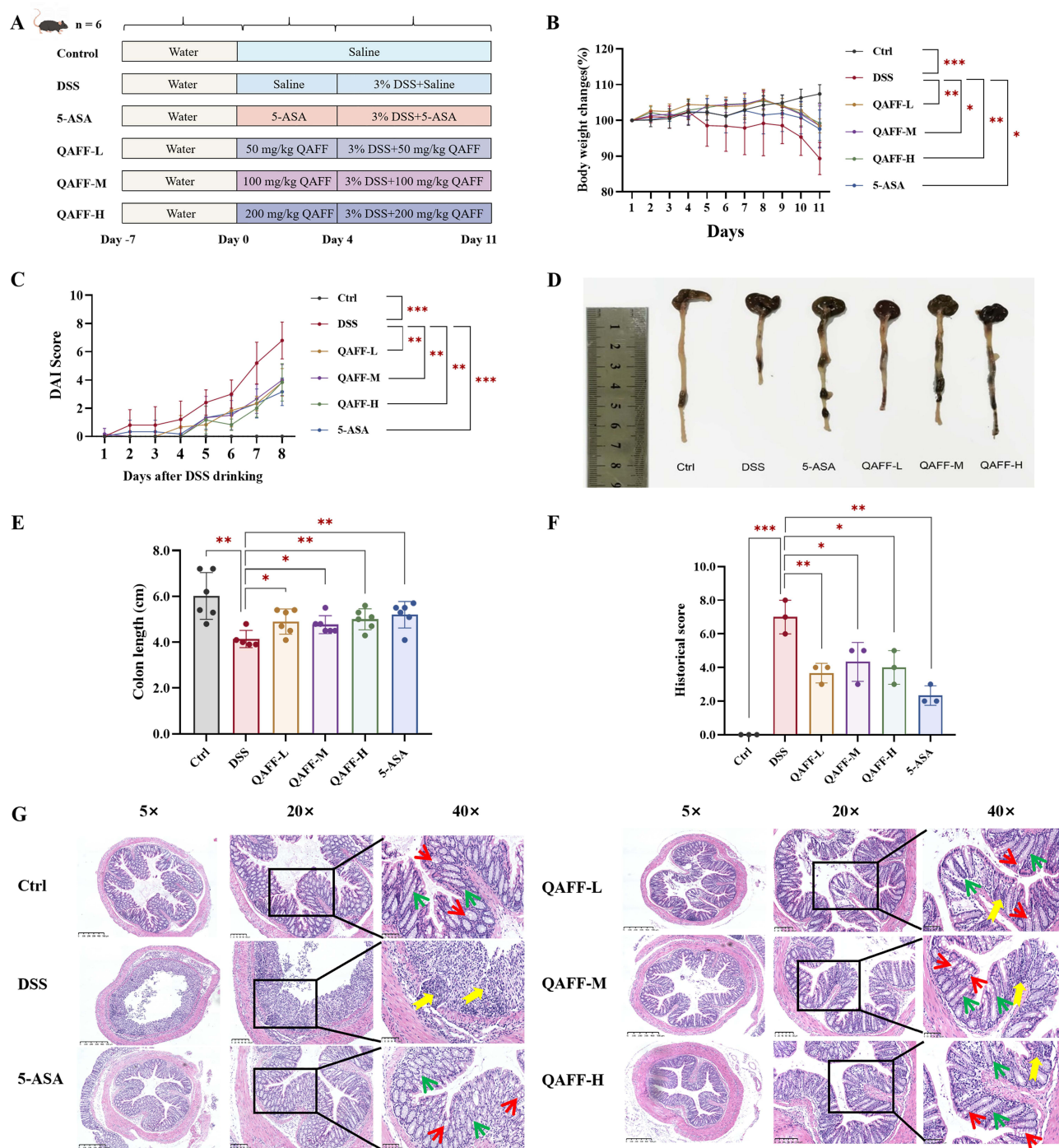


Figure 2 QAFF dampened DSS-induced UC mice. (A) The designed chart of in vivo experiment. (B) The changes in body weight ($n = 6$). (C) DAI Score ($n = 6$). (D) The representative colonic appearance. (E) Colonic length (unit: cm) ($n = 6$). (F) Histological scores of colons in each group ($n = 3$). (G) Colonic H&E staining. Red arrow represents the goblet cells. Green arrow represents the crypts. Yellow arrow represents inflammatory infiltration. Data are expressed as mean \pm SD. * $P < 0.05$, ** $P < 0.01$, and *** $P < 0.001$ vs DSS group.

weight loss, severe rectal bleeding, reduced stool volume, elevated DAI, and shortened colon length. Conversely, the groups receiving varying doses of QAFF and 5-ASA demonstrated a significant reversal of weight loss, lower DAI scores, and preserved colon length ($P < 0.05$, $P < 0.01$; Figure 2B–E). Furthermore, histological analysis revealed that QAFF treatment decreased mucosal necrosis and reduced inflammatory cell infiltration, resulting in lower histological colitis scores than the DSS group (Figure 2F and G). Collectively, these findings indicate that QAFF effectively attenuated DSS-induced acute UC and ameliorated associated symptoms. This study highlights the potential therapeutic value of QAFF in colitis management.

QAFF Inhibited the Production of Pro-Inflammatory Cytokines in DSS-Induced UC Mice

Pro-inflammatory cytokines are closely related to the pathogenesis of colitis.²³ To investigate their involvement, we employed the ELISA method for quantifying the concentrations of IL-6, TNF- α , and IL-1 β in colon tissues. The results demonstrated that the DSS-exposed group significantly elevated the levels of these inflammatory mediators in colon tissues, in comparison to the untreated Ctrl group ($P < 0.05$, $P < 0.01$) (Figure 3A–C). Notably, administering varying QAFF dosages resulted in significant reductions in these cytokines, approaching the efficacy observed in the 5-ASA group. These findings suggest that QAFF effectively attenuated inflammatory responses in the colons of DSS-treated mice with UC, thereby highlighting its potential therapeutic value due to its anti-inflammatory properties.

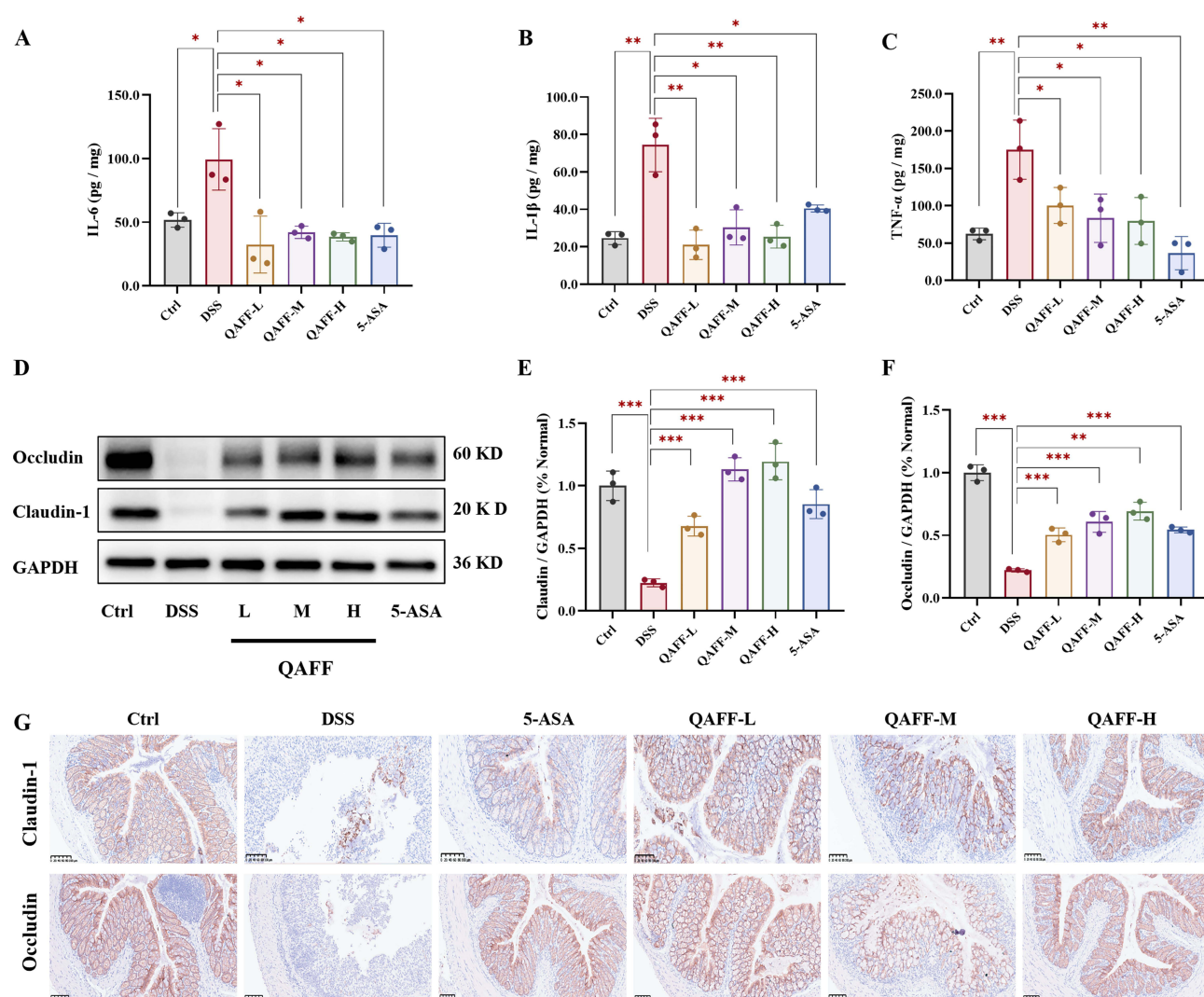


Figure 3 QAFF inhibited colonic inflammation and restored the intestinal barrier in DSS-exposed UC mice. (A–C) Levels of IL-6, IL-1 β , and TNF- α in colon tissues of colitis mice. (D–F) Expression of Claudin-1 and Occludin (E and F) in the colon of mice. (G) Representative immunohistochemical staining of Claudin-1 and Occludin in the colon of colitis mice. Scale bar, 100 μ m. Data are expressed as mean \pm SD ($n = 3$). * $P < 0.05$, ** $P < 0.01$, and *** $P < 0.001$ vs DSS group.

QAFF Restored the Integrity of Colonic Epithelial Barrier in DSS-Induced UC Mice

The tight junction (TJ) plays a key role in maintaining the integrity of intestinal barrier, safeguarding the organism from harmful substances within the gut.²⁴ To assess the protective impact of QAFF on the colonic epithelial barrier in mice, Western blotting was employed to monitor the alterations in the levels of Claudin-1 and Occludin proteins. The results demonstrated a substantial reduction in these protein expressions in the DSS group ($P < 0.001$), indicating a disruption of the intestinal barrier due to DSS exposure. However, QAFF administration resulted in differential upregulation of these expressions, contributing to maintaining the colonic epithelial barrier (Figure 3D–F) ($P < 0.01$, $P < 0.001$). Immunohistochemical analysis was performed to corroborate these findings in representative samples from each group. These findings corroborated the Western blot analysis, demonstrating decreased expressions of Claudin-1 and Occludin in the DSS group compared to the Ctrl group, with an evident reversal trend after QAFF treatment (Figure 3G). In summary, QAFF enhanced the integrity of the colonic epithelial barrier by upregulating the expression of Claudin-1 and Occludin proteins.

Identification of Potential Pathways Through Transcriptomics

To elucidate the mechanism of action of QAFF treatment for UC, we employed RNA sequencing analysis to identify genome-wide transcriptional changes in the mouse colon. PCA revealed distinct clustering of the Ctrl, DSS, and QAFF-L groups, indicating substantial differences with good reproducibility in gene expression profiles (Figure 4A). A volcano plot was generated, depicting a total of 1582 DEGs in the DSS group in comparison to the Ctrl group, with 1348 genes upregulated and 234 genes downregulated (Figure 4B). In contrast, the QAFF-L group exhibited only 34 upregulated and 34 downregulated genes (Figure 4C and Table S5). KEGG pathway enrichment analysis revealed that QAFF treatment impacted several pathways, including p53 signaling, MAPK pathway, PI3K/AKT signaling pathway, and other related pathways (Figure 4D and Table S6). To further investigate the expression of the enriched pathways at the overall level for all genes, GSEA was further performed. The entire PI3K/AKT pathway gene set revealed that DSS treatment induced a significant upregulation compared to the Ctrl group (NES: 1.8, $P < 0.001$, and FDR: 0.004). Conversely, QAFF-L administration resulted in a downregulation of the PI3K/AKT pathway gene set compared to the DSS group (NES: -1.47, P : 0.003, and FDR: 0.101) (Figure 4E and F). These results suggested that QAFF may exert therapeutic effects in UC, potentially through downregulation of the PI3K/AKT pathway.

QAFF Mitigated Inflammation Through Inhibition of the PI3K/AKT Pathway

Western blotting analysis was further performed to confirm the key regulatory proteins within the PI3K/AKT pathways, guided by the transcriptome analysis. To validate the regulatory effects of QAFF, the expression levels of total and phosphorylated proteins involved in this pathway were examined. As depicted in Figure 4, the results indicate a significant elevation in the phosphorylated protein levels of PI3K (P-PI3K, Figure 4G and H) and AKT (P-AKT, Figure 4G, I, and K) in the DSS group relative to the Ctrl group ($P < 0.05$, $P < 0.01$), while the protein levels of AKT were not affected among these groups (Figure 4J). This suggested that PI3K/AKT signaling pathway was activated following DSS treatment. However, the middle and high dosages of QAFF treatment downregulated the activation of this signaling pathway induced by DSS, as demonstrated by the inhibition of their phosphorylation. These findings suggested that QAFF attenuated DSS-induced colonic damage probably by suppressing the PI3K/AKT signaling pathway, providing valuable insight into a potential therapeutic target for the intervention in UC.

QAFF Restored the Composition and the Abundance of the Gut Microbiome in DSS-Induced UC Mice

16S rRNA gene sequencing was conducted to assess the impact of QAFF on the gut microbiota within cecal contents, with a focus on the QAFF-L group in comparison to the DSS group. Initially, the Chao1 index and observed species richness were decreased in DSS-treated mice in comparison to the Ctrl group. In contrast, both the 5-ASA and QAFF-L group displayed increase in Alpha diversity metrics, but there was no significant difference in QAFF-L compared with DSS group (Figure 5A and B). The PCoA plots indicated distinct clustering patterns, separating the Ctrl and DSS groups.

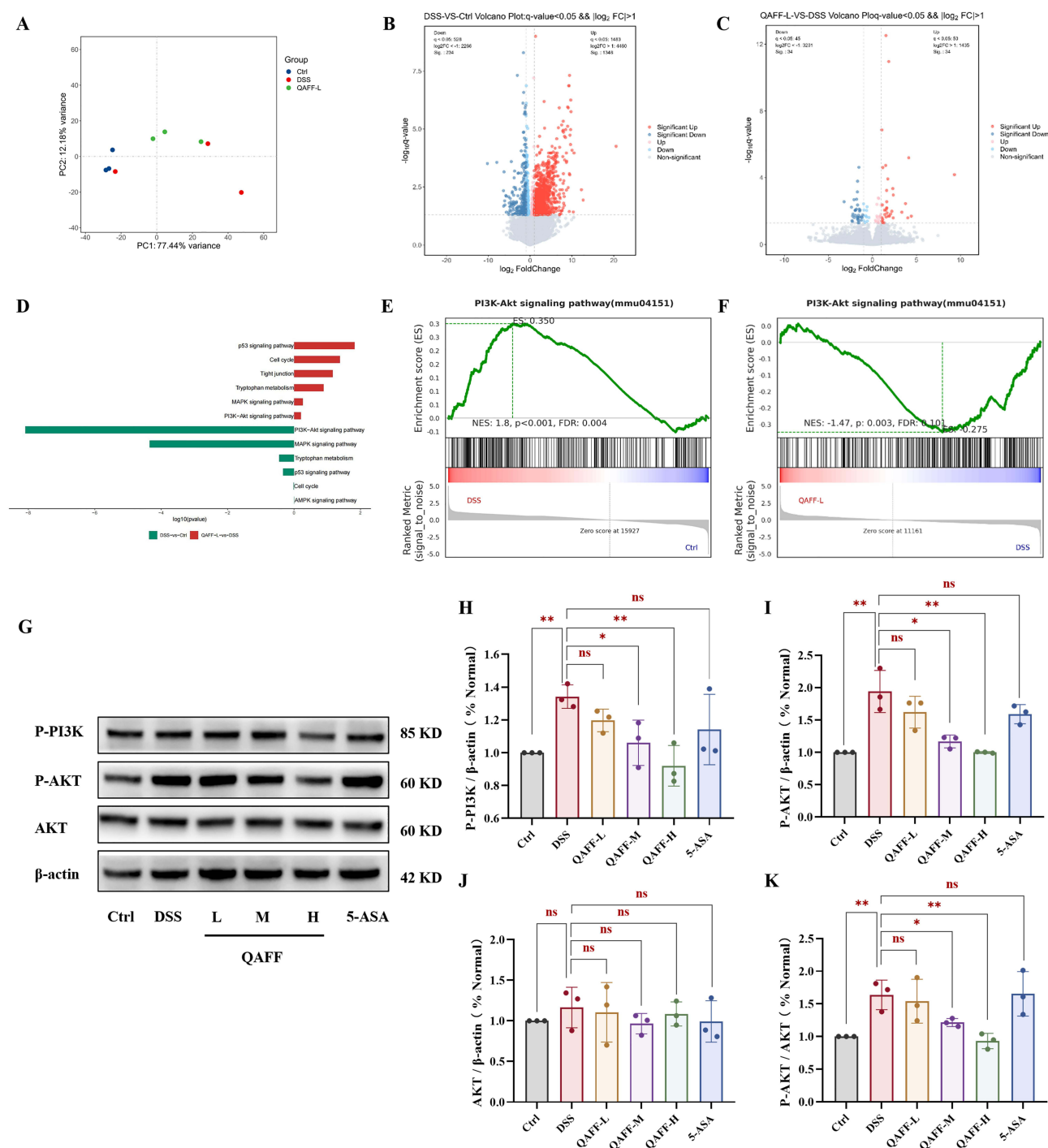


Figure 4 Transcriptomics analysis results and QAFF inhibited the expression of PI3K/AKT pathway. **(A)** PCA analysis. **(B and C)** Volcano plots analysis ($q < 0.05$, $|\log_2 FC| > 1$). DSS vs Ctrl **(B)**. QAFF-L vs DSS **(C)** (down-blue, up-red). **(D)** KEGG pathway enrichment of differential gene expression among Ctrl, DSS, and QAFF-L. **(E and F)** GSEA analysis of PI3K/AKT signaling pathway. DSS vs Ctrl **(E)**. QAFF-L vs DSS **(F)**. **(G–K)** Protein expressions of P-PI3K **(H)**, P-AKT **(I)**, AKT **(J)**, and P-AKT/AKT **(K)**. Data are expressed as mean \pm SD ($n = 3$). * $P < 0.05$, ** $P < 0.01$, and ns = not significant vs DSS group.

Notably, the microbial community structure of the QAFF-L group clustered closer to the Ctrl group, demonstrating a clear distinction from the DSS group (Figure 5C). To gain a deeper understanding of the structural changes within gut microbiota, we conducted an analysis of the relative abundance of bacterial taxa at both the phylum and genus levels, utilizing histograms for visualization. At the phylum level (Figure 5D), DSS-induced colitis resulted in a notable increase in the abundance of *Firmicutes* and *Proteobacteria* compared with Ctrl group, while concurrently decreasing the

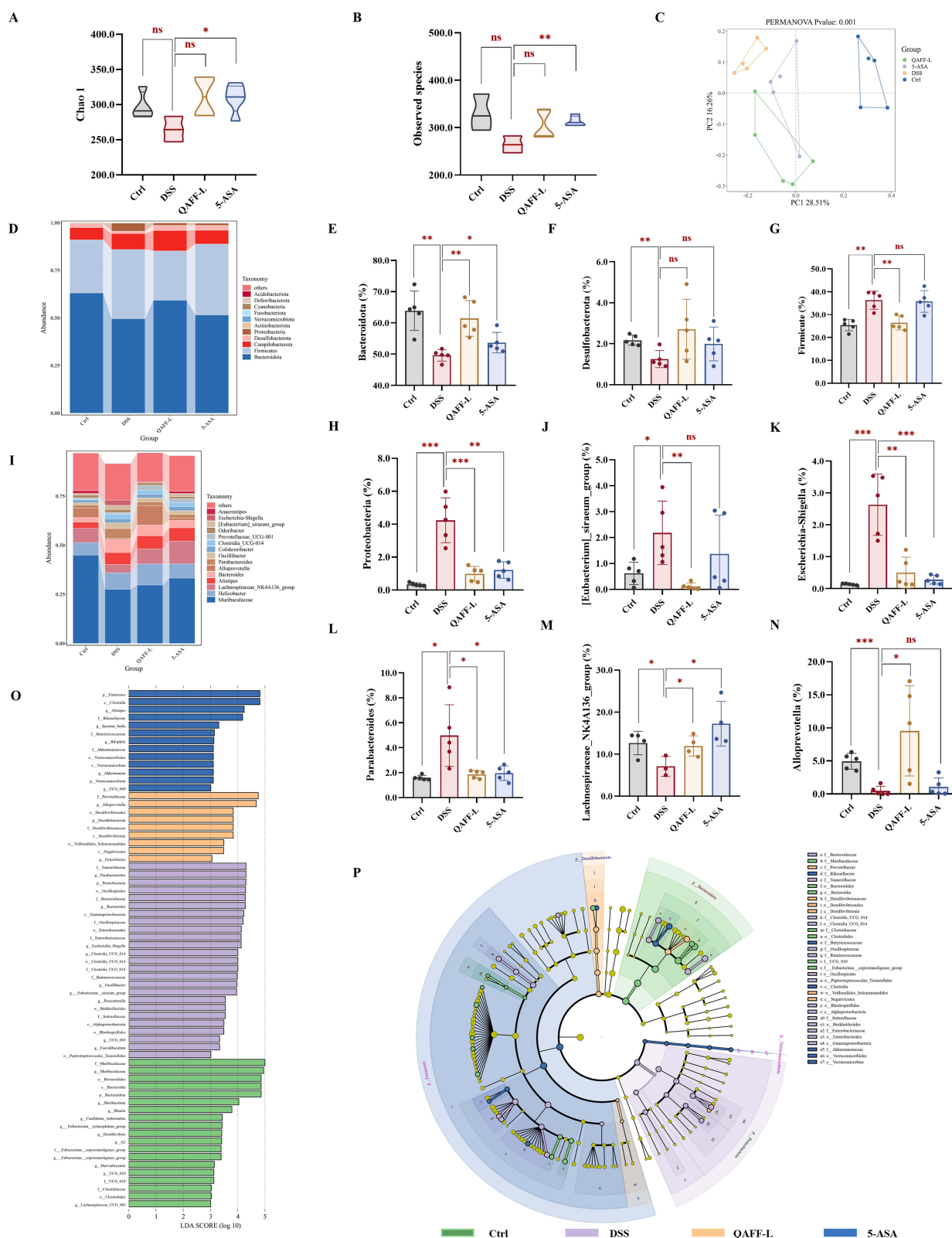


Figure 5 QAFF restored the gut microbiome in vivo. (**A** and **B**) Alpha-diversity of gut microbiome in mice of Chao I index (**A**), and Observed species (**B**). Depicting the gut microbiome β -diversity by PCoA (**C**). (**D**–**H**) Relative abundance at the phylum level (**D**) including Bacteroidota (**E**), Desulfobacterota (**F**), Firmicute (**G**), and Proteobacteria (**H**). (**I**–**N**) Relative abundance of species at the genus level (**I**) including *Eubacterium_siraeum_group* (**J**), *Escherichia-Shigella* (**K**), *Parabacteroides* (**L**), *Lachnospiraceae_NK4A136_group* (**M**), and *Alloprevotella* (**N**). (**O** and **P**) Effects of QAFF on biomarker taxa assessed by LEfSe. Histogram (**O**) and Cladogram (**P**) of LDA score ($n = 3$ – 5). * $P < 0.05$, ** $P < 0.01$, *** $P < 0.001$, and ns = not significant vs DSS group.

abundance of *Bacteroidota* and *Desulfobacterota*, findings that are consistent the previous research.⁹ Notably, treatment with both QAFF-L and 5-ASA increased the abundance of *Bacteroidota* and *Desulfobacterota*, while simultaneously mitigating the levels of *Firmicutes* and *Proteobacteria*, reversing the DSS-induced changes (Figure 5E–H). At the genus level (Figure 5I), DSS treatment significantly increased the abundance of *[Eubacterium]_siraenum_group*, *Escherichia-Shigella*, and *Parabacteroides*, with a decrease in *Lachnospiraceae_NK4A136_group* and *Alloprevotella*. Interestingly, QAFF treatment restored the abundance of all investigated genera to levels comparable to the control group (Figure 5J–N and Tables S7–S12).

This rigorous identification of the dominant and characteristic bacteria was further performed through LEfSe analysis (Figure 5O and P). The resulting cladogram depicts the linear discriminant analysis (LDA) scores for taxa with varying abundance levels. LEfSe analysis identified a total of 66 taxa, spanning phylum to genus, with 19 taxa enriched in the control group, 25 taxa in the DSS group, 9 taxa in the QAFF group, and 13 taxa in the 5-ASA group (Table S13). Notably, the control group exhibited a significantly higher abundance of *Bacteroidia*, *Muribaculaceae*, *Blautia*, *Prevotellaceae_NK3B31_group*, and *Eubacterium_xylanophilum_group*. Conversely, the DSS group was characterized by the enrichment of genera such as *Parabacteroides*, *Oscillibacter*, *Escherichia-Shigella*, *Clostridia_UCG_014*, and *Eubacterium_siraenum_group*. Following QAFF treatment, a marked elevation in the abundance of *Alloprevotella*, *Prevotellaceae*, *Enterobacter*, and *Desulfovibrionales* was observed. Consistent with aforementioned results, the LEfSe analysis was successfully applied to identify specific bacterial biomarkers associated with each gut microbiota composition. In conclusion, QAFF treatment exhibited promising potential for UC treatment through modulation of the intestinal microbiota.

QAFF Tempered Metabolomics in DSS-Induced UC Mice

To study the endogenous metabolites associated with QAFF-mediated therapeutic efficacy, non-targeted metabolomic analyses of colon tissues were conducted using UPLC-MS/MS. As shown in Figure 6A, the PLS-DA model demonstrated significant cluster differentiation among the Ctrl, DSS, and QAFF-L groups, exhibiting good reproducibility for samples in each group. A total of 244 metabolites were identified differentially between the DSS and Ctrl groups, with 96 being up-regulated and 148 down-regulated (Figure 6B and Table S14). In contrast, the QAFF-L and DSS groups exhibited 66 upregulated metabolites and 60 downregulated metabolites, totaling 126 differential metabolites (Figure 6C and Table S15). We identified 34 shared metabolites that were expressed in both the DSS versus Ctrl and QAFF-L versus DSS comparisons using Venn diagrams (Figure 6D). Notably, 19 of these metabolites were indicative of reversal of metabolic disturbances induced by DSS after QAFF-L administration (Table S16). These include phosphatidylethanolamine (PE), phosphatidylcholine (PC), phosphatidyl serine (PS), and glycerophospholipid-related metabolites such as Glycerophosphoric acid, PC (18:3(6Z,9Z, 12Z)/0:0), PS(O-18:0/0:0), PE(O-16:0/0:0), and PC (P -16:0/22:6 (5Z,7Z,10Z,13Z,16Z,19Z)-OH(4)) (Figure 6E).

The analysis of the potential pathways involving these shared differential metabolites revealed that most of these pathways are associated with lipid metabolisms, including Glycerophospholipid metabolism, Linoleic acid metabolism, and Glycerolipid metabolism. Among them, Glycerophospholipid metabolism was significantly enriched in the including QAFF-L versus DSS versus Ctrl (Figure 6F). Furthermore, GSEA of the entire Glycerophospholipid metabolism pathway gene set indicated significant down-regulation (NES: -2.02, $P < 0.001$, FDR: 0.014) in the DSS treatment group compared to the Ctrl, whereas QAFF-L administration led to upregulation on this pathway compared to the DSS group (NES: 1.99, $P < 0.001$, FDR: 0.017) (Figure 6G and H). These findings suggest that QAFF-L may primarily restore DSS-induced metabolic disorders by regulating Glycerophospholipid metabolism.

Spearman Correlation Analysis

Correlation Between Gut Microbiota and Indicative Evaluations

Spearman correlation analysis was conducted to evaluate the associations between the differential gut microbiota in QAFF-L versus DSS versus Ctrl groups, colitis symptoms, inflammatory responses (including inflammatory factors and PI3K/AKT pathway), and TJs (Figure 7A). The findings demonstrated a positive correlation between the *Lachnospiraceae_NK4A136_group* and both colon length and TJs while exhibiting a negative correlation with DAI,

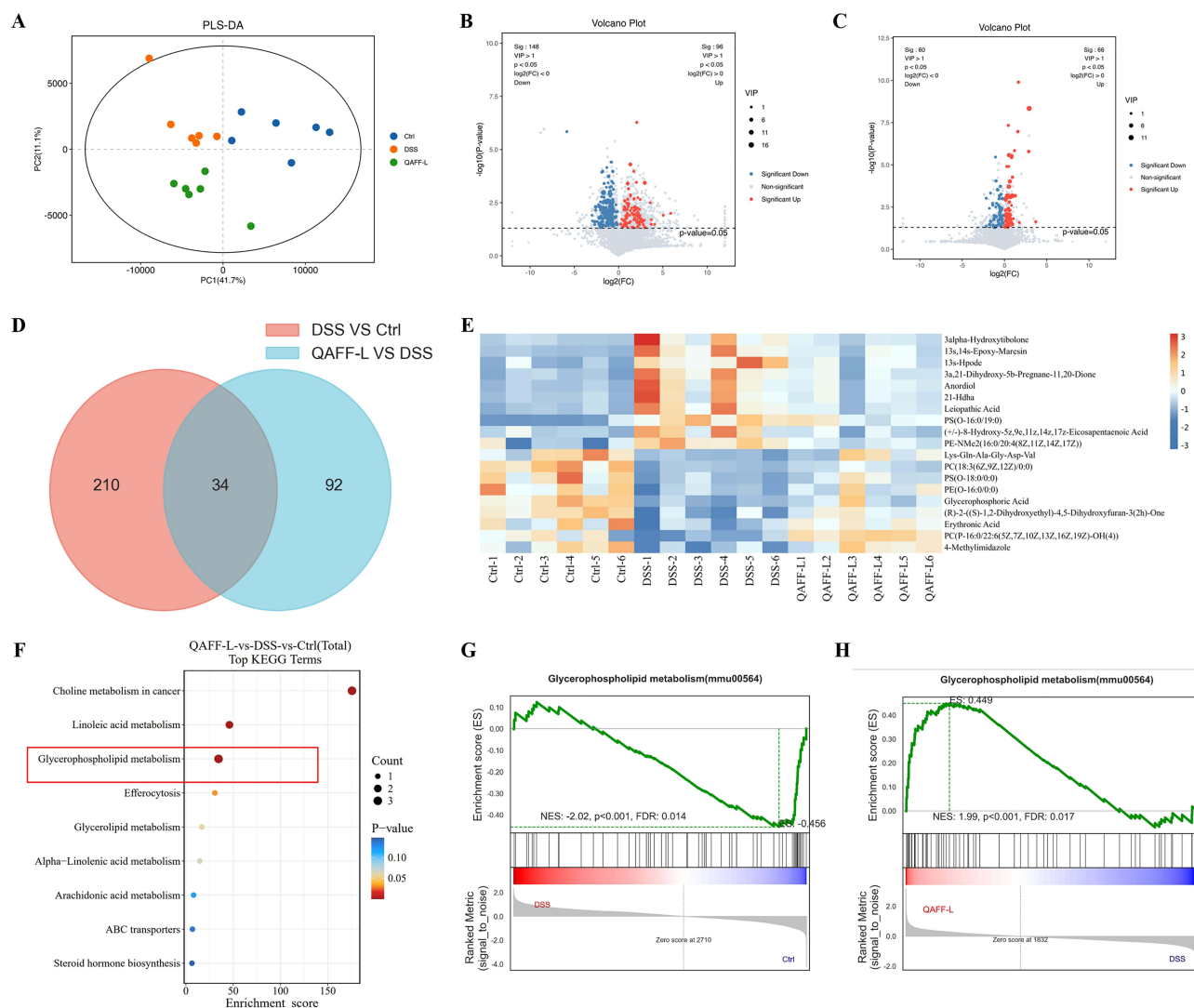


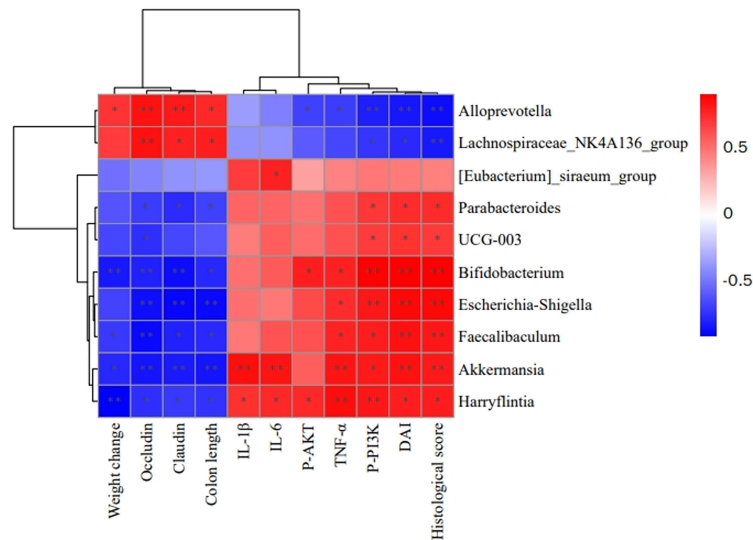
Figure 6 QAFF tempered metabolomics in DSS-induced UC mice. **(A)** The PLS-DA analysis. **(B and C)** Volcano plots analysis ($P < 0.05$, $VIP > 1$). DSS vs Ctrl **(B)**. QAFF-L vs DSS **(C)** (down–blue, up–red). **(D)** Common differential metabolites between QAFF-L vs DSS vs Ctrl. **(E)** Heatmap of common differential metabolites. **(F)** KEGG pathway enrichment of common differential metabolites among Ctrl, DSS, and QAFF-L. Highlighted with the red box. **(G and H)** GSEA analysis of Glycerophospholipid metabolism signaling pathway. DSS vs Ctrl **(G)**. QAFF-L vs DSS **(H)**. Data are expressed as mean \pm SD ($n = 6$).

histological score, and P-AKT. *Alloprevotella* exhibited a stronger correlation, being positively linked to body weight and negatively associated with P-PI3K and TNF- α . On the contrary, *Escherichia-Shigella* revealed positive connections with DAI, histological score, and inflammatory response, whereas negative associations with colon length and TJs. *[Eubacterium]_siraum_group* primarily showed a positive correlation with IL-6. These data suggested that QAFF-L may function as an anti-colitis agent by modulating specific gut microbiota.

Correlation Between Metabolites and Gut Microbiota

Spearman correlation analysis was further employed to clarify the potential correlations between microbial genera and colonic metabolites after QAFF-L treatment (Figure 7B). These results indicated that phospholipid metabolites, including PC (P-16:0/22:6(5Z,7Z,10Z,13Z,16Z,19Z)-OH(4)), PE (O-16:0/0:0), and PS (O-18:0/0:0), were positively correlated with the dominant bacterium *Alloprevotella* ($P < 0.01$, $P < 0.05$) but negatively correlated with the *[Eubacterium]_siraum_group* and *Faecalibaculum*. It suggested that *Alloprevotella* actively responded to QAFF-L treatment and may enhance lipid metabolism, such as PC and PE, in DSS-induced UC mice. Additionally, Glycerophosphoric acid demonstrated a highly negative correlation with *Escherichia-Shigella* and *Parabacteroides* ($P < 0.01$), indicating that

A



B

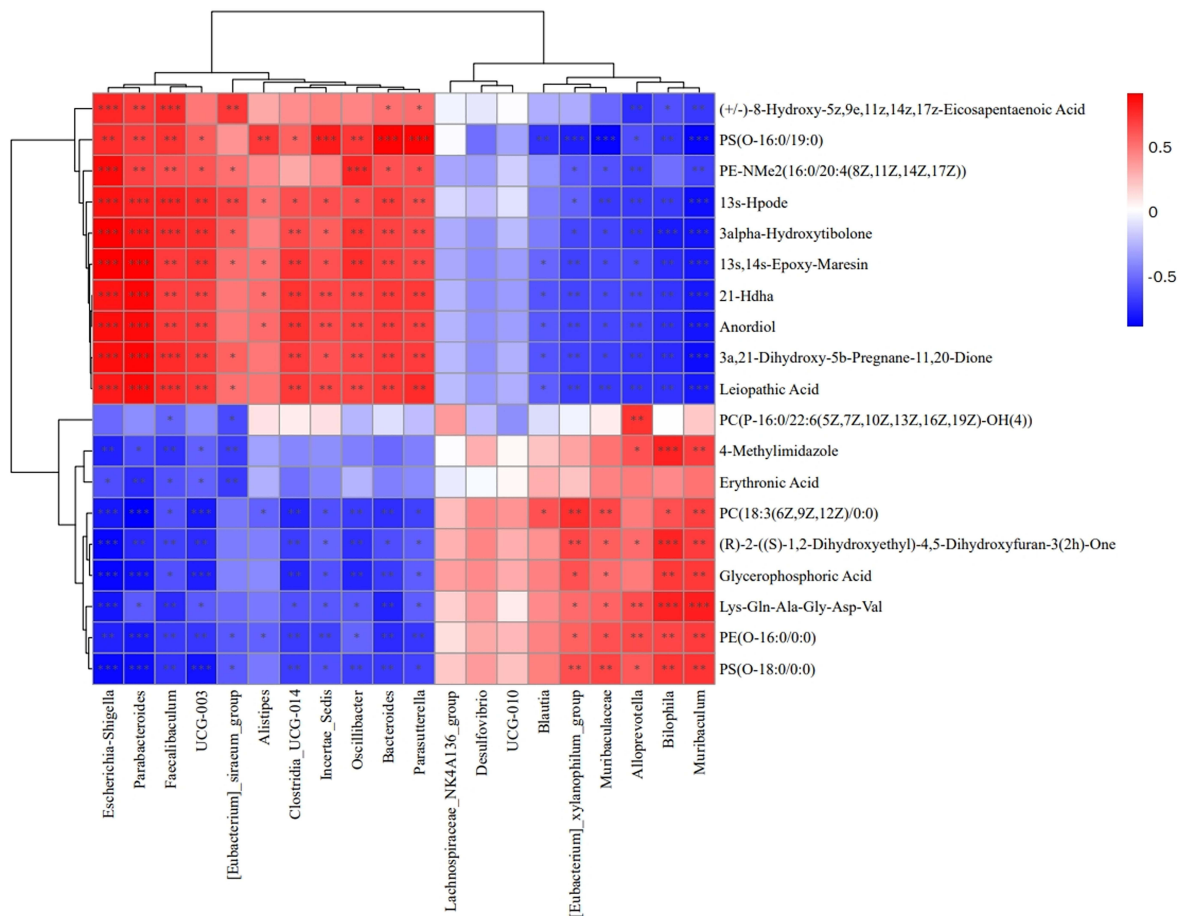


Figure 7 Heat map of the Spearman correlation analysis. **(A)** The correlation between the key gut microbiota modulated by QAFF-L and indicative evaluations in UC. **(B)** The correlation between endogenous metabolites and QAFF-L-modulated gut microbiota. *P < 0.05, **P < 0.01, and ***P < 0.001.

these bacteria may disrupt phospholipid structures. Therefore, these results suggest that phospholipid metabolites may be involved in the therapeutic efficacy of QAFF on DSS-induced colitis by modulating the gut microbiota.

FMT of QAFF Ameliorated DSS-Induced UC Mice

To evaluate the efficacy of the QAFF-modulated gut microbiota in mitigating colitis, FMT was performed in mice with 3% DSS-induced colitis (recipients) after antibiotic pretreatment. The donors for FMT were mice previously treated with either QAFF or DSS (Figure 8A). Compared to recipient mice transplanted with DSS-derived fecal microbiota (DSS + DSSfe), those

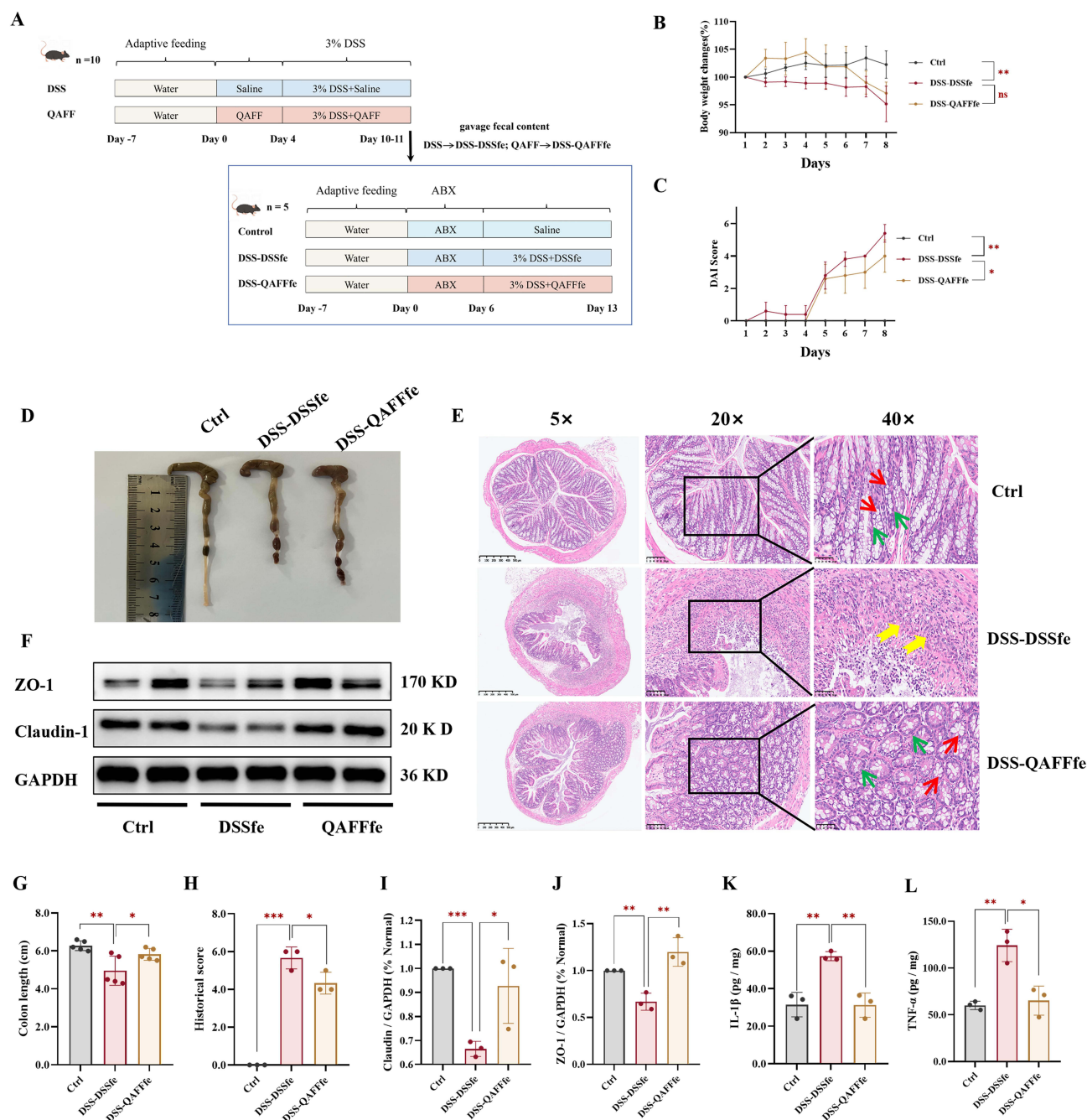


Figure 8 FMT of QAFF ameliorated DSS-induced UC mice. **(A)** The precise diagram for FMT. **(B)** The changes in body weight (n = 5). **(C)** DAI Scores (n = 5). **(D)** The characteristic appearance of colon. **(E)** H&E staining of colon. Red arrow represents the goblet cells. Green arrow represents the crypts. Yellow arrow represents inflammatory infiltration. **(F)** Expression of claudin-1 and ZO-1 proteins in the colon of mice. **(G)** Colonic length (unit: cm) (n = 5). **(H)** Histological scores of colons in each group (n = 3). **(I and J)** Quantitative expression of claudin-1 and ZO-1 (n = 3). **(K and L)** Colon tissue levels of IL-1 β , and TNF- α in mice with colitis (n = 3). Data are expressed as mean \pm SD. * P < 0.05, ** P < 0.01, *** P < 0.001, and ns = not significant vs DSS-DSSfe group.

receiving QAFF-derived fecal microbiota (DSS + QAFFfe) exhibited a slower rate of weight loss, normalization of DAI scores, colon length, and histological features (Figure 8B–E, G and H). Furthermore, FMT significantly restored the integrity of the intestinal barrier, particularly in the expression of proteins claudin-1 and ZO-1, in mice with colitis (Figure 8F, I and J). In addition, FMT led to a significant reduction in the levels of the inflammatory factors TNF- α and IL-1 β within colonic tissues (Figure 8K and L), indicating a strong anti-inflammatory effect. These results confirm that gut microbiota is essential for the UC efficacy of QAFF-L treatment.

Discussion

Quzhou Aurantii Fructus has been used as a folk medicine in the treatment of chronic gastritis and peptic ulcer. Notably, the total flavonoids of QAF have shown potential as a promising therapeutic candidate for mitigating inflammatory responses associated with acute lung injury, ovalbumin (OVA)-induced allergic asthma, non-alcoholic fatty liver disease, and related metabolic diseases.²⁵ These are achieved by targeting multiple signaling pathways, including MAPK, NF- κ B, and AMPK signaling pathways.²⁶ Furthermore, administration of total flavonoids of QAF could increase the protein expression in intestinal tight junction and improve the damage of intestinal mucosal barrier caused by nonsteroidal anti-inflammatory drugs (NSAID) over a long period.²⁷ The primary constituents of QAF are flavanone and their glycosides. QAFF was separated from QAF by purification and then identified using LC-MS/MS analysis. The contents of four key compounds—naringin, neohesperidin, narirutin, and hesperidin — were determined to be 361.0, 353.0, 42.2, and 32.8 mg/g, respectively, with the contents of total flavonoids over 70%. Interestingly, studies have shown that Aurantii Fructus Immaturus (AFI) flavonoid, which includes 10% naringin and 8% neohesperidin, not only reduces inflammatory response but also modulates gut microbiota in DSS-treated UC mice.^{28,29} This prompted us to consider whether QAFF possesses anti-UC properties. It is worthy to study it and further elucidate its mechanism of action in UC treatment, offering a basis for broadening the clinical application of QAFF.

To rigorously investigate the pharmacological effects and underlying mechanisms of action of QAFF in UC treatment, an *in vivo* experiment was conducted. The DSS-induced colitis mouse model closely replicates key immunological and histopathological features observed in UC patients, making it a well-established and representative model.^{30,31} In this study, mice were orally administered 3% DSS to assess the impact of QAFF on inflammation and intestinal barrier function in the context of UC. Mice in the treatment groups received the dose of 50, 100, and 200 mg/kg of QAFF in 0.2 mL of sterile saline, equivalent to 0.60, 1.20, and 2.40 g QAF/kg, respectively. The middle dose of QAFF was approximately equivalent to the adult clinical dose (7.32 g QAF for a 75 kg person) recorded in “Zhejiang Traditional Chinese Medicine Processing Norms (2015 Edition)”.³² The DSS group exhibited significant weight loss, increased DAI scores, colon shortening, elevated pathological scores, and notable inflammatory infiltration, confirming the successful establishment of the DSS-induced UC mouse model on the final day of the experiment. Compared with the DSS group, QAFF at various concentrations of 50, 100, and 200 mg/kg showed efficacy in ameliorating symptoms of UC in mice.

During the initial stages of UC, pro-inflammatory cytokines produced by innate immune cells, particularly IL-1 β , TNF- α , and IL-6, predominate.²³ Elevated levels of pro-inflammatory cytokines, such as IL-1 β and IFN- γ , in UC can disrupt intestinal barrier function, leading to increased permeability and exacerbation of inflammation.³³ In the present study, QAFF markedly decreased the levels of IL-6, IL-1 β and TNF- α in colonic tissues, compared to the DSS group. The results were consistent with those observations from AFI flavonoid treatment, where the expression of these cytokines was reduced in the colon of UC mice, as determined by qPCR assay.²⁸ Deficiencies in TJ proteins, such as Claudins, Occludin, ZO proteins, and junctional adhesion molecules, contribute to the clinical manifestations observed in the intestinal mucosa of IBD patients.³⁴ Claudins and Occludin play key roles in the formation and disassembly of TJs, particularly important for the paracellular flux of small molecules.³⁵ In this study, QAFF administration selectively upregulated the expression levels of Claudin-1 and Occludin in UC mice by Western blotting, as further confirmed by immunohistochemistry. These findings indicate that QAFF may exert its therapeutic effects in UC through anti-inflammatory activities and preservation of the integrity of intestinal barrier.

To further elucidate the underlying mechanisms by which QAFF exerts its therapeutic effects in UC mice, we employed transcriptomic analysis in colon tissue. GSEA revealed that DSS administration potential upregulated the overall expression of the PI3K/AKT signaling pathway, while this effect was subsequently attenuated by QAFF treatment. To verify the regulation of this signaling pathway, our *in vivo* experiments demonstrated that QAFF effectively

treated DSS-induced UC by suppressing the phosphorylated protein levels of PI3K and AKT by Western blotting. Consistent with our findings, numerous studies have demonstrated that experimental models of colitis indeed exhibit aberrant activation of the PI3K/AKT pathway, which can be countered by treatment with various herbal medicines.³⁶ For example, Kuiyu Pingchang Decoction (KYPCD), Quzhou Aurantii Fructus as a primary constituent, has been shown to modulate the MAPK, PI3K/AKT, IL-17, and HIF-1 pathways in UC treatment and to act on the PI3K pathway in the treatment of upper respiratory tract infections.³⁷ The flavonoids of *Lonicera rupicola* Hook.f.et Thoms showed comprehensive protective effects in DSS-induced UC mice, reducing inflammation and oxidative stress, improving epithelial barrier integrity, and modulating the gut microenvironment through inhibition the PI3K/AKT pathway.³⁰ Therefore, these findings indicate that PI3K/AKT pathway modulated by QAFF treatment may represent a new therapeutic target for the intervention in UC.

The gut microbiota, dominated by *Firmicutes* and *Bacteroidota*, plays a critical role in human health.³⁸ Patients with UC exhibit a significantly lower abundance of *Bacteroidota* compared to healthy controls, during both active and remission phases of the disease.³⁹ Additionally, abnormal expansion of *Proteobacteria* disrupts gut microbiota balance, thereby promoting the development of intestinal diseases.⁴⁰ In this study, the low-dose of QAFF, which exhibited minimal efficacy differences among these groups, was chosen for further mechanistic exploration into its effects on intestinal microbial regulation. The findings indicated that the administration of DSS to mice significantly reduced alpha diversity within the gut microbiota and increased the relative abundance of *Firmicutes* and *Proteobacteria*, while concurrently decreasing the abundance of *Bacteroidota*. Notably, treatment with 50 mg/kg of QAFF effectively alleviated these compositional imbalances within the gut microbiota. At the genus level, QAFF significantly enhanced the abundance of *Lachnospiraceae_NK4A136_group* and *Alloprevotella*, while simultaneously decreased the abundance of *Escherichia-Shigella*. *Lachnospiraceae_NK4A136_group*, belonging to the *Firmicutes* phylum, has been reported to produce butyric acid and sodium butyrate, which alleviate UC symptoms.⁴¹ Importantly, sodium butyrate has been shown to ameliorate inflammatory response and intestinal barrier dysfunction by downregulating the AKT and NF- κ B p65 signaling pathways through hepatic microsomal cytochrome P450 2A5.⁴² Furthermore, *Alloprevotella* increases the production of short-chain fatty acids, particularly propionate, which in turn modulates acetylation to inhibit Th17 differentiation and reduce inflammatory cytokines secreted by pathogenic Th17 cells.⁴³ In contrast, *Escherichia-Shigella*, a member of the *Proteobacteria* phylum, is positively correlated with UC severity.⁴⁴ It is known to promote macrophage apoptosis and IL-1 β release and exhibits a strong correlation with IL-6 levels in UC patients.^{45,46} Summarily, the regulation of gut microbiota and their potential effects on UC are crucial for the treatment of UC by QAFF. The relationship between the gut microbiome and symptoms in UC, inflammation responses, tight junction proteins, and PI3K/AKT pathway has been effectively correlated using Spearman correlation (Figure 7A). These findings suggest that QAFF may ameliorate intestinal inflammation and the intestinal barrier in UC mice by restoring the balance of the gut microbiome. To confirm this hypothesis, FMT was further performed and the results verified this effect (Figure 8).

In recent years, the changes in mucosal lipids have been used to screen patients with UC as an evaluative indicator of disease status.⁴⁷ Lipid profiling of feces and serum revealed that altered levels of four lipid markers (phosphocholine, ceramides, sphingomyelins, and triglycerides) accurately predicted the anti-TNF response in UC patients.⁴⁸ Studies have shown that supplementation with PC34:1 could treat DSS-induced UC mice by increasing fumaric acid content in the mouse colon.⁴⁹ From our results, QAFF up-regulated glycerophosphoric acid, PC (18:3(6Z,9Z, 12Z)/0:0), PC (P-16:0/22:6(5Z,7Z,10Z,13Z,16Z,19Z)-OH(4)), PS (O-18:0/0:0), PE (O-16:0/ 0:0), and other glycerophospholipid -related metabolites to restore DSS-induced metabolic disorders. The results of GSEA analysis indicate that QAFF may restore DSS-induced UC mice by regulating Glycerophospholipid metabolism. Further Spearman correlation analysis suggested that these phospholipid metabolites were closely associated with those microbiome modulations by QAFF, particularly showing positive correlations with *Alloprevotella* and negative correlations with the *[Eubacterium]_siraeum_group* and *Faecalibaculum*. These findings suggest that the gut microbiota-metabolite axis may be involved in the anti-UC effects of QAFF. Collectively, we provide novel insights into the mechanisms of action of anti-UC and therapeutical agents, which will promote the exploration and utilization of QAFF. However, additional studies are necessary to unravel the precise mechanism underlying the modulation of gut microbiome and its metabolites in relation to the anti-UC effect of QAFF. Furthermore, it remains unknown whether main active compounds or compounds combination exist in QAFF for the treatment of UC, and further safety and efficacy verification needs to be carried out.

Conclusion

QAFF was found to alleviate symptoms of colitis, suppress the levels of pro-inflammatory cytokines, repair the integrity of intestinal barrier, and suppress the activation of PI3K/AKT pathway in mice with DSS-induced UC. Furthermore, QAFF was observed to restore the disrupted gut microbiome, a result that was corroborated by FMT. Collectively, these findings highlight the substantial protective effects of QAFF on UC and indicate its potential as a therapeutic strategy in UC treatment.

Abbreviations

QAF, Quzhou Aurantii Fructus; QAFF, Quzhou Aurantii Fructus Flavonoids; UC, ulcerative colitis; IBD, inflammatory bowel disease; DSS, dextran sulfate sodium; DAI, disease activity index; UPLC-MS/MS, ultra-performance liquid chromatography-tandem mass spectrometry; H&E, hematoxylin and eosin staining; KEGG, Kyoto Encyclopedia of Genes and Genomes; GO, Gene Ontology; IL-1 β , interleukin-1 β ; IL-6, interleukin-6; TNF- α , tumor necrosis factor- α ; ZO-1, zonula occludens-1; PI3K, Phosphoinositide 3-kinase; AKT, protein kinase B; JAK, the Janus kinase; STAT, signal transducer and activator of transcription, MAPK, mitogen-activated protein kinase; NF- κ B, nuclear factor- κ B; GSEA, Gene Set Enrichment Analysis; PCoA, principal coordinate analysis; PVDF, Polyvinylidene difluoride; SDS-PAGE, sodium dodecyl sulfate-polyacrylamide gel electrophoresis; TBST, Tris-buffered-saline solution and Tween 20; PLS-DA, partial least squares discriminant analysis; PE, phosphatidylethanolamine; PC, phosphatidylcholine; PS, phosphatidyl serine; FMT, fecal microbiota transplantation; ABX, Antibiotics.

Data Sharing Statement

The data that support the findings of this study are available from the corresponding author, upon reasonable request.

Ethics Approval and Consent to Participate

All animal experiments in this study received approval from the Institutional Animal Care and Ethics Committee of Hangzhou Medical College (No. 2024-039).

Consent for Publication

All authors reviewed and approved the final manuscript.

Author Contributions

All authors made a significant contribution to the work reported, whether that is in the conception, study design, execution, acquisition of data, analysis and interpretation, or in all these areas; took part in drafting, revising or critically reviewing the article; gave final approval of the version to be published; have agreed on the journal to which the article has been submitted; and agree to be accountable for all aspects of the work.

Funding

This research was supported by the Traditional Chinese Medicine project of Zhejiang Provincial Health Commission (2024ZL369), Basic and Public Welfare Research Program of Zhejiang Province (LZ24H280006), the Special Project of Zhejiang Academy of Medical Sciences (YS2022006), Zhejiang Province Traditional Chinese Medicine Science and Technology Project (2021ZX004), Scientific and Technological Innovation (Xinmiao Talents) Program of Zhejiang Province (2023R425011), and Key Discipline of Zhejiang Province in Public Health and Preventive Medicine (First Class, Category A), Hangzhou Medical College.

Disclosure

The authors assert that they possess no recognizable conflicting monetary concerns or individual connections that may have seemed to impact the research detailed in this manuscript.

References

- Conrad K, Roggenbuck D, Laass MW. Diagnosis and classification of ulcerative colitis. *Autoimmun Rev*. 2014;13(4–5):463–466. doi:10.1016/j.autrev.2014.01.028
- Ng SC, Shi HY, Hamidi N, et al. Worldwide incidence and prevalence of inflammatory bowel disease in the 21st century: a systematic review of population-based studies. *Lancet*. 2017;390(10114):2769–2778. doi:10.1016/S0140-6736(17)32448-0
- Gajendran M, Loganathan P, Jimenez G, et al. A comprehensive review and update on ulcerative colitis. *Dis Mon*. 2019;65(12):100851. doi:10.1016/j.disamonth.2019.02.004
- Gros B, Kaplan GG. Ulcerative colitis in adults: a review. *JAMA*. 2023;330(10):951–965. doi:10.1001/jama.2023.15389
- Porter RJ, Kalla R, Ho GT. Ulcerative colitis: recent advances in the understanding of disease pathogenesis. *F1000Res*. 2020;9:F1000FacultyRev–294. doi:10.12688/f1000research.20805.1
- Zheng S, Xue T, Wang B, Guo H, Liu Q. Chinese medicine in the treatment of ulcerative colitis: the mechanisms of signaling pathway regulations. *Am J Chin Med*. 2022;50(7):1781–1798. doi:10.1142/S0192415X22500756
- Marchesi JR, Adams DH, Fava F, et al. The gut microbiota and host health: a new clinical frontier. *Gut*. 2016;65(2):330–339. doi:10.1136/gutjnl-2015-309990
- Hu Y, Chen Z, Xu C, Kan S, Chen D. Disturbances of the gut microbiota and microbiota-derived metabolites in inflammatory bowel disease. *Nutrients*. 2022;14(23):5140. doi:10.3390/nu14235140
- Zhang SL, Wang SN, Miao CY. Influence of microbiota on intestinal immune system in ulcerative colitis and its intervention. *Front Immunol*. 2017;8:1674. doi:10.3389/fimmu.2017.01674
- Zhang H, Wang Y, Su Y, Fang X, Guo W. The alleviating effect and mechanism of Bilobalide on ulcerative colitis. *Food Funct*. 2021;12(14):6226–6239. doi:10.1039/D1FO01266E
- Wang HO, Li JY, Huang WK, Ye YP, Gao LJ. The regulation of intestinal microbiota and the intervention of Chinese herbal medicine in the treatment of ulcerative colitis. *Pharmacol Res Mod Chin Med*. 2024;10:100356. doi:10.1016/j.prmcm.2024.100356
- Tursi A, D'Avino A, Brandimarte G, et al. Enhancing oral 5-ASA effectiveness in mild-to-moderate ulcerative colitis through an *H. erinaceus*-based nutraceutical add-on multi-compound: the “HERICIUM-UC” two-arm multicentre retrospective study. *Pharmaceutics*. 2024;16(9):1133. doi:10.3390/pharmaceutics16091133
- Hu YH, Liu J, Li H, Tang W, Li XW, Guo YW. Chemical constituents from *Citrus changshan-huyou* and their anti-inflammatory activities. *Chem Biodivers*. 2020;17(11):e2000503. doi:10.1002/cbdv.202000503
- Bai YF, Wang SW, Wang XX, et al. The flavonoid-rich Quzhou Fructus Aurantii extract modulates gut microbiota and prevents obesity in high-fat diet-fed mice. *Nutr Diabetes*. 2019;9(1):30. doi:10.1038/s41387-019-0097-6
- Zhang QX, Song WY, Tao GQ, et al. Comparison of chemical compositions and antioxidant activities for the immature fruits of *Citrus changshan-huyou* Y.B. Chang and *Citrus aurantium* L. *Molecules*. 2023;28(13):5057. doi:10.3390/molecules28135057
- Manicassamy S, Manoharan I. Mouse models of acute and chronic colitis. *Methods mol Biol*. 2014;1194:437–448. doi:10.1007/978-1-4939-1215-5_25
- Obermeier F, Kojouharoff G, Hans W, Schölmerich J, Gross V, Falk W. Interferon-gamma (IFN-gamma)- and tumour necrosis factor (TNF)-induced nitric oxide as toxic effector molecule in chronic dextran sulphate sodium (DSS)-induced colitis in mice. *Clin Exp Immunol*. 1999;116(2):238–245. doi:10.1046/j.1365-2249.1999.00878.x
- Xu Y, Wang X, Han D, et al. Revealing the mechanism of Jiegeng decoction attenuates bleomycin-induced pulmonary fibrosis via PI3K/Akt signaling pathway based on lipidomics and transcriptomics. *Phytomedicine*. 2022;102:154207. doi:10.1016/j.phymed.2022.154207
- Subramanian A, Tamayo P, Mootha VK, et al. Gene set enrichment analysis: a knowledge-based approach for interpreting genome-wide expression profiles. *Proc Natl Acad Sci U S A*. 2005;102(43):15545–15550. doi:10.1073/pnas.0506580102
- Han Z, Jin J, Chen X, He Y, Sun H. Adjuvant activity of tubeimosides by mediating the local immune microenvironment. *Front Immunol*. 2023;14:1108244. doi:10.3389/fimmu.2023.1108244
- Wu M, Li P, An Y, et al. Phloretin ameliorates dextran sulfate sodium-induced ulcerative colitis in mice by regulating the gut microbiota. *Pharmacol Res*. 2019;150:104489. doi:10.1016/j.phrs.2019.104489
- Li Q, Cui Y, Xu B, et al. Main active components of Jiawei Gegen Qinlian decoction protects against ulcerative colitis under different dietary environments in a gut microbiota-dependent manner. *Pharmacol Res*. 2021;170:105694. doi:10.1016/j.phrs.2021.105694
- Nakase H, Sato N, Mizuno N, Ikawa Y. The influence of cytokines on the complex pathology of ulcerative colitis. *Autoimmun Rev*. 2022;21(3):103017. doi:10.1016/j.autrev.2021.103017
- Otani T, Furuse M. Tight junction structure and function revisited. *Trends Cell Biol*. 2020;30(10):805–817. doi:10.1016/j.tcb.2020.08.004
- Gao L, Zhang H, Yuan CH, et al. *Citrus aurantium* ‘Changshan-huyou’-An ethnopharmacological and phytochemical review. *Front Pharmacol*. 2022;13:983470. doi:10.3389/fphar.2022.983470
- Li L, Chen J, Lin L, et al. Quzhou Fructus Aurantii Extract suppresses inflammation via regulation of MAPK, NF-κB, and AMPK signaling pathway. *Sci Rep*. 2020;10(1):1593. doi:10.1038/s41598-020-58566-7
- Chen ZY, Li JS, Jiang JP, Yan MX, He BH. Effect of pure total flavonoids from citrus on hepatic SIRT1/PGC-1α pathway in mice with NASH. *Zhongguo Zhong Yao Za Zhi*. 2014;39(1):100–105. doi:10.4268/cjcm20140120
- Chen SY, Zhou QY, Chen L, Liao X, Li R, Xie T. The *Aurantii Fructus Immaturus* flavonoid extract alleviates inflammation and modulate gut microbiota in DSS-induced colitis mice. *Front Nutr*. 2022;9:1013899. doi:10.3389/fnut.2022.1013899
- Tong L, Zhou D, Gao J, Zhu Y, Sun H, Bi K. Simultaneous determination of naringin, hesperidin, neohesperidin, naringenin and hesperetin of *Fructus aurantii* extract in rat plasma by liquid chromatography tandem mass spectrometry. *J Pharm Biomed Anal*. 2012;58:58–64. doi:10.1016/j.jpba.2011.05.001
- Li C, Wang L, Zhao J, et al. *Lonicera rupicola* Hook.f.et Thoms flavonoids ameliorated dysregulated inflammatory responses, intestinal barrier, and gut microbiome in ulcerative colitis via PI3K/AKT pathway. *Phytomedicine*. 2022;104:154284. doi:10.1016/j.phymed.2022.154284
- Alex P, Zachos NC, Nguyen T, et al. Distinct cytokine patterns identified from multiplex profiles of murine DSS and TNBS-induced colitis. *Inflamm Bowel Dis*. 2009;15(3):341–352. doi:10.1002/ibd.20753

32. Tian M, Huang W, Chen J, et al. The extract from Quzhou Aurantii Fructus attenuates cough variant asthma through inhibiting the TRPV1/Ca²⁺/NFAT/TSLP pathway and ferroptosis via TRPV1 mediation in ovalbumin-induced mice. *J Ethnopharmacol.* **2025**;338(Pt 1):119038. doi:10.1016/j.jep.2024.119038
33. Kaminsky LW, Al-Sadi R, Ma TY. IL-1 β and the intestinal epithelial tight junction barrier. *Front Immunol.* **2021**;12:767456. doi:10.3389/fimmu.2021.767456
34. Gassler N, Rohr C, Schneider A, et al. Inflammatory bowel disease is associated with changes of enterocytic junctions. *Am J Physiol Gastrointest Liver Physiol.* **2001**;281(1):G216–G228. doi:10.1152/ajpgi.2001.281.1.G216
35. Van Itallie CM, Anderson JM. Claudins and epithelial paracellular transport. *Annu Rev Physiol.* **2006**;68:403–429. doi:10.1146/annurev.physiol.68.040104.131404
36. Ma Y, Lang X, Yang Q, et al. Paoniflorin promotes intestinal stem cell-mediated epithelial regeneration and repair via PI3K-AKT-mTOR signalling in ulcerative colitis. *Int Immunopharmacol.* **2023**;119:110247. doi:10.1016/j.intimp.2023.110247
37. Wen Y, Wang X, Si K, Xu L, Huang S, Zhan Y. Exploring the mechanisms of self-made Kuiyu Pingchang recipe for the treatment of ulcerative colitis and irritable bowel syndrome using a network pharmacology-based approach and molecular docking. *Curr Comput Aided Drug Des.* **2023**;20(5):534–550. doi:10.2174/1573409919666230515103224
38. Andoh A. Physiological role of gut microbiota for maintaining human health. *Digestion.* **2016**;93(3):176–181. doi:10.1159/000444066
39. Zhou Y, Zhi F. Lower level of Bacteroides in the gut microbiota is associated with inflammatory bowel disease: a meta-analysis. *Biomed Res Int.* **2016**;2016:5828959. doi:10.1155/2016/5828959
40. Shin NR, Whon TW, Bae JW. Proteobacteria: microbial signature of dysbiosis in gut microbiota. *Trends Biotechnol.* **2015**;33(9):496–503. doi:10.1016/j.tibtech.2015.06.011
41. Wu Y, Ran L, Yang Y, et al. Deferasirox alleviates DSS-induced ulcerative colitis in mice by inhibiting ferroptosis and improving intestinal microbiota. *Life Sci.* **2023**;314:121312. doi:10.1016/j.lfs.2022.121312
42. Satka S, Frybortova V, Zapletalova I, et al. Effect of DSS-induced ulcerative colitis and butyrate on the cytochrome P450 2A5: contribution of the microbiome. *Int J mol Sci.* **2022**;23(19):11627. doi:10.3390/ijms231911627
43. Han B, Shi L, Bao MY, et al. Dietary ellagic acid therapy for CNS autoimmunity: targeting on Alloprevotella rava and propionate metabolism. *Microbiome.* **2024**;12(1):114. doi:10.1186/s40168-024-01819-8
44. Kojima A, Nakano K, Wada K, et al. Infection of specific strains of Streptococcus mutans, oral bacteria, confers a risk of ulcerative colitis. *Sci Rep.* **2012**;2:332. doi:10.1038/srep00332
45. Mirsepasi-Lauridsen HC, Vallance BA, Krogfelt KA, Petersen AM. Escherichia coli pathobionts associated with inflammatory bowel disease. *Clin Microbiol Rev.* **2019**;32(2):e00060–18. doi:10.1128/CMR.00060-18
46. Liu JL, Gao YY, Zhou J, et al. Changes in serum inflammatory cytokine levels and intestinal flora in a self-healing dextran sodium sulfate-induced ulcerative colitis murine model. *Life Sci.* **2020**;263:118587. doi:10.1016/j.lfs.2020.118587
47. Diab J, Hansen T, Goll R, et al. Lipidomics in ulcerative colitis reveal alteration in mucosal lipid composition associated with the disease state. *Inflamm Bowel Dis.* **2019**;25(11):1780–1787. doi:10.1093/ibd/izz098
48. Vich Vila A, Zhang J, Liu M, Faber KN, Weersma RK. Untargeted faecal metabolomics for the discovery of biomarkers and treatment targets for inflammatory bowel diseases. *Gut.* **2024**;1–12. doi:10.1136/gutjnl-2023-329969
49. Yu T, Zhou Z, Liu S, et al. The role of phosphatidylcholine 34:1 in the occurrence, development and treatment of ulcerative colitis. *Acta Pharm Sin B.* **2023**;13(3):1231–1245. doi:10.1016/j.apsb.2022.09.006

Journal of Inflammation Research

Publish your work in this journal

The Journal of Inflammation Research is an international, peer-reviewed open-access journal that welcomes laboratory and clinical findings on the molecular basis, cell biology and pharmacology of inflammation including original research, reviews, symposium reports, hypothesis formation and commentaries on: acute/chronic inflammation; mediators of inflammation; cellular processes; molecular mechanisms; pharmacology and novel anti-inflammatory drugs; clinical conditions involving inflammation. The manuscript management system is completely online and includes a very quick and fair peer-review system. Visit <http://www.dovepress.com/testimonials.php> to read real quotes from published authors.

Submit your manuscript here: <https://www.dovepress.com/journal-of-inflammation-research-journal>

Dovepress
Taylor & Francis Group